A 17 year time series of ground-based GNSS for sensing of atmospheric water vapour

A 17 YEAR TIME SERIES OF GROUND-BASED GNSS FOR SENSING OF ATMOSPHERIC WATER VAPOUR

Tong Ning[1] **and Gunnar Elgered**[2]

[1] *Lantmäteriet, SE-801 82, Gävle, Sweden*
[2] *Chalmers University of Technology, Onsala Space Observatory, SE-439 92 Onsala, Sweden*

ABSTRACT

We have analysed 17 years of GPS data from 123 sites in Europe and obtained time series of the amount of Integrated Water Vapour (IWV) in the atmosphere. In total 69 sites have data from a period longer than 10 years and 35 sites have data from more than 15 years. Two different data analyses have been carried out to study the impact of the use of different models. We find that the impact is small, but the IWV results from different data analyses shall not be mixed when studying the long term stability of the IWV, e.g. when estimating trends. Using the IWV results from the analysis using the more recent models we estimate linear trends as well as the amplitude and the phase of the diurnal signal in the IWV at the different sites. The estimated trends are sensitive to different periods analysed and are comparable to the corresponding uncertainties. The estimated amplitude of the diurnal cycle during the summer varies from 0.16 kg/m^2 to 1.46 kg/m^2 while the peak time of the hourly IWV mean is around 18 local solar time for the most of sites.

Key words: water vapour, time series, climate.

1. INTRODUCTION

Due to the importance of water vapour to the Earth's climate system [1], it is of great interest to monitor the long-term change in the Integrated Water Vapour (IWV) in the atmosphere.

It is well known that the IWV can be derived from observations acquired from Global Navigation Satellite Systems (GNSS), e.g., the Global Positioning System (GPS). The advantages of using GNSS are that the observations acquired from the ground can be made during all weather conditions, with a high temporal resolution (a few minutes), and with a high reliability.

The homogeneity of the time series of the GNSS-derived IWV is affected by data processing-related changes, i.e. inconsistencies due to updates of the reference frame and applied models, implementation of a different elevation cutoff angle, different mapping functions, and other differences in the processing strategies. Steigenberger et al. [2] found that such changes can cause inconsistencies of several millimetres in the GNSS-derived tropospheric delay time series. In order to significantly reduce these processing-related inconsistencies, a homogenous reprocessing of the whole GNSS data time series is necessary.

2. DATA ANALYSIS

A previously studied data set of 14 years of GPS measurements [3] has been extended by three years and covers the time period from 1 January 1997 to 31 December 2013. In total, 69 sites have time series longer than 10 years. These sites are located between latitudes 39 °N and 71 °N, and between longitudes −22 °E and +31 °E. In addition to this extended IWV time series the entire data set has been reprocessed. Table 1 lists the details about the two processings. Both were performed using GIPSY with the precise point positioning (PPP) strategy. Differences in the new processing compared to the earlier one are that up-to-date models are applied. The Niell mapping function (NMF) [4] was replaced by the Vienna 1 mapping function (VMF) [5], corrections for higher-order ionospheric effects was introduced [6], and ambiguities were resolved. The sites with a data coverage of more than ten years were used in the study (see

Table 1. Models used in the GPS data analyses.

Model	Old analysis	New analysis
GPS software	GIPSY v5.0	GIPSY v6.2
Mapping funct.	NMF	VMF
Elev. cutoff	10°	10°
Ocean loading	FES 2004 [7]	FES 2004 [7]
Antenna PCV	igs05_1604.atx	igs08_1740.atx
Ambiguity res.	No	Yes
Ionosphere	Standard	2nd order (IGRF)

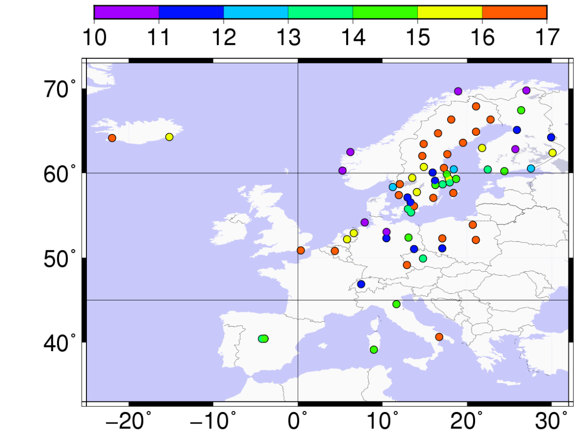

Figure 1. The 69 sites studied with IWV time series longer than ten years. The colour of the site marker indicates the length of the time series (in years).

Figure 1).

3. RESULTS

The mean value of the IWV, obtained from the new reprocessed data, varies over Europe which is illustrated in Figure 2. It is evident that the sites located at low latitudes have higher IWV than the ones located at high latitudes.

3.1. Comparison between the two data analyses

The difference in the IWV caused by the adoption of each of updates was investigated for two sites, Onsala and Matera, using the all 17 years data. The first line in Table 2 shows the mean IWV and the trend for the old processing. Thereafter the NMF was replaced by the VMF (2nd line), the second order ionospheric model was introduced (3rd line), and finally the ambiguity resolution was added (4th line). Both stations show similar results when comparing the IWV between the old and the new processing. Typical IWV mean differences are around 0.1 kg/m^2.

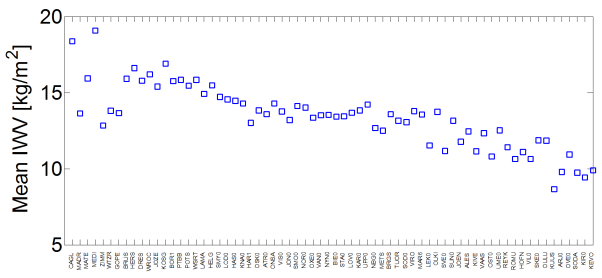

Figure 2. IWV mean values for the 69 sites having more than 10 years of data. The sites are sorted by increasing latitude.

The differences between the two processings are less than 0.04 kg/(m$^2\cdot$ decade) in the resulted trend.

Finally we compared the amplitudes of the diurnal cycle, using data only from the summer seasons (June, July, and August), in the IWV from two data analyses (not shown). A maximum difference of 0.05 kg/m^2 is seen in the amplitude of the diurnal cycle while the difference in the phase is within ± 2 h. In the following, all results are obtained only from the new processing.

3.2. Linear trends in the IWV

Estimated linear trends in the IWV over the time period 1997–2013 are in the range from -0.8 kg/(m$^2\cdot$ decade) to +0.6 kg/(m$^2\cdot$ decade), see Figure 3. These trends are presented for the 35 sites having more than 15 years of data. The uncertainties are rescaled in order to be consistent with the misfit of the model as described in [8] and are in the range 0.2–0.5 kg/(m$^2\cdot$ decade). We note that they are comparable to the values of the trend.

In order to investigate the sensitivity of the trends to the selected time period, the trends are also estimated for each season. The trend values with their uncertainties are presented in Table 3 and in Figure 4. Large differences are noted between the seasons. The largest trends are seen during the summer seasons.

3.3. Diurnal components in the IWV

The diurnal cycle, driven by the radiation from the sun, is an expected and well known signal in the IWV. Given its high temporal resolution, GPS-derived IWV is an efficient tool to evaluate the ability of Numerical Weather Prediction Models (NWP) to simulate the diurnal cycle [9].

We investigated the diurnal signal calculating the mean IWV for each hour (local solar time). As seen in Figure 5 the variation is close to a sine function, although significant deviations are seen for the four example sites.

In order to study the stability of the diurnal signal over the years we calculated the amplitude and the phase averaged over periods of 1, 3, and 5 years. The result is shown for the same four example sites in Figure 6 by fitting a sine function to the data. It is clear that both the amplitude and the phase averaged over only 1 year are highly variable and the results starts to be stable when the averaging time is longer.

Figure 7 summarise the results of the amplitude of the diurnal signal for all 69 sites with data covering at least 10 years. The estimated amplitude is varying from 0.16 kg/m^2 to 1.46 kg/m^2. In general an increase of the amplitude is seen when the latitude decrease.

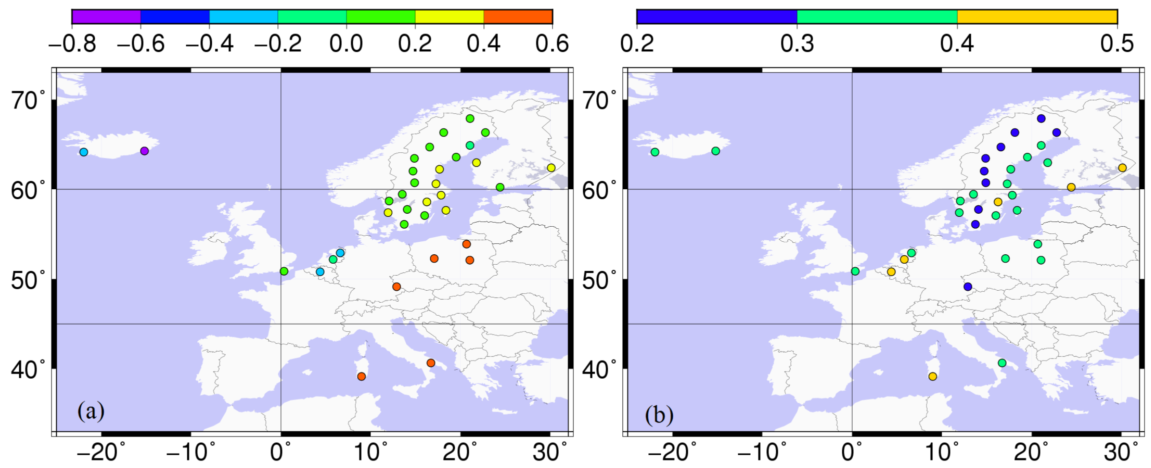

Figure 3. Linear trends estimated for the IWV for the period 1997–2013 (a) and their respective uncertainties (b). The IWV value is colour coded in the unit kg/(m^2 · decade).

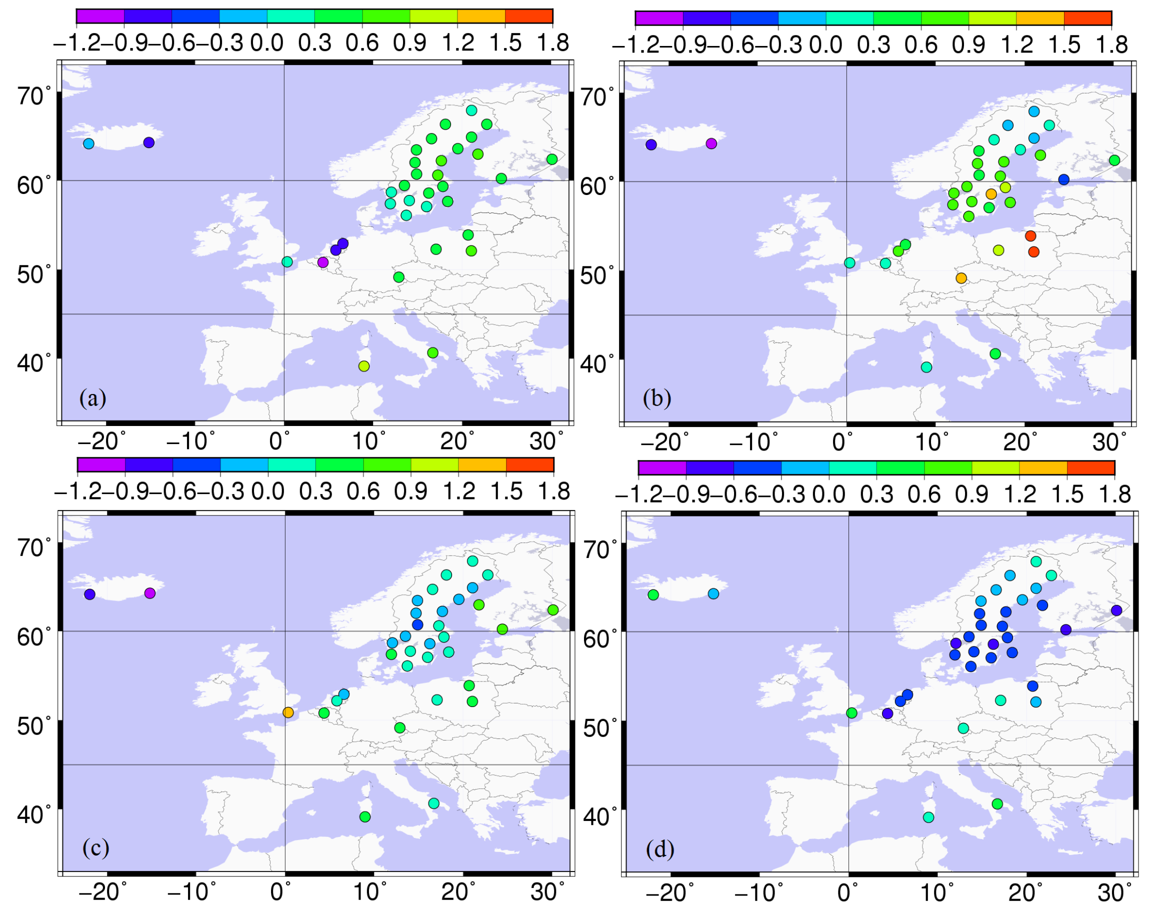

Figure 4. Linear trends estimated for the IWV for the different seasons for period 1997–2013, spring (MAM) (a), summer (JJA) (b), autumn (SON) (c) and winter (DJF) (d). The IWV value is colour coded in the unit kg/(m^2 · decade).

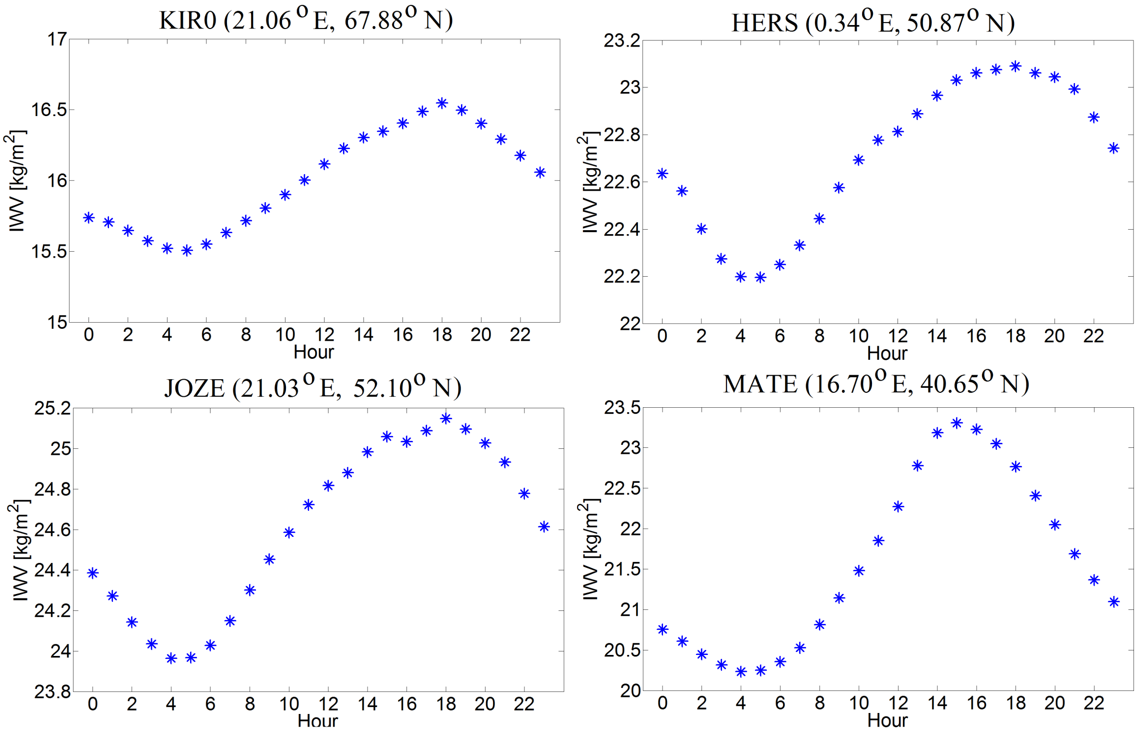

Figure 5. The diurnal amplitude in the IWV presented as hourly means.

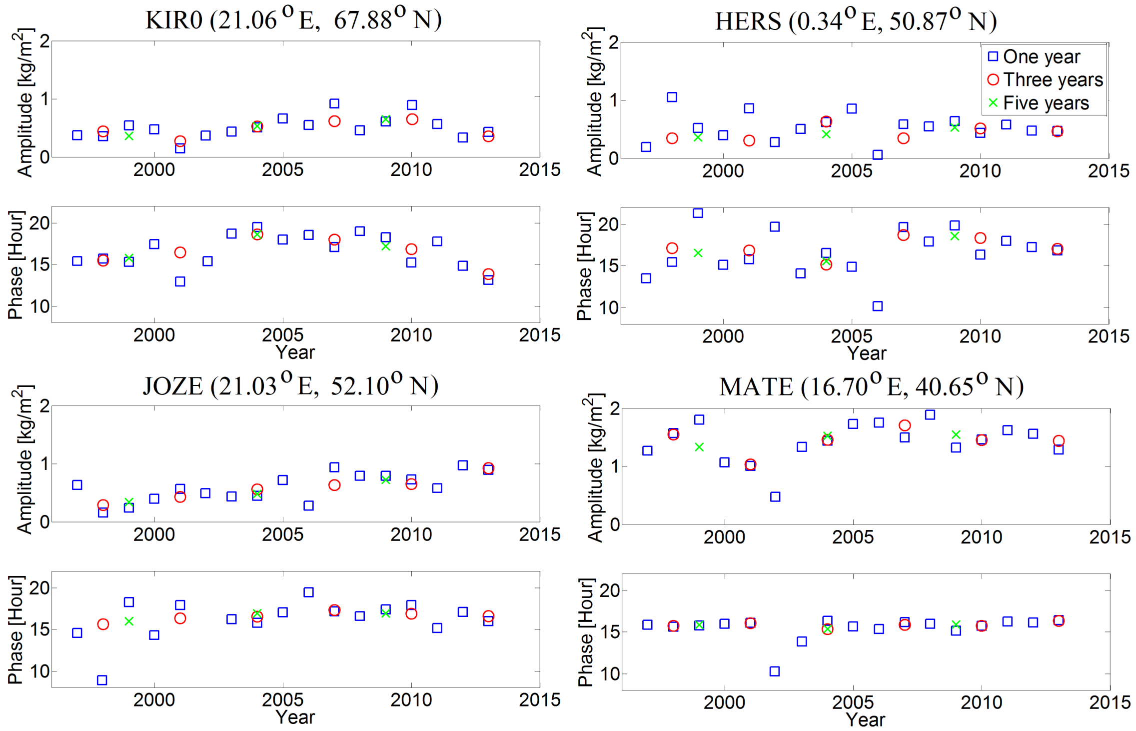

Figure 6. The amplitude and the phase of the diurnal cycle estimated for the summer months (JJA) and averaged over 1, 3, and 5 years for the same four example sites as in Figure 5.

Table 2. Impact on the IWV at Onsala and Matera due to model changes in the analysis.

Model	Onsala		Matera	
	Mean	Trend	Mean	Trend
	kg/m^2	$kg/(m^2 \cdot decade)$	kg/m^2	$kg/(m^2 \cdot decade)$
NMF	14.01	0.28	15.71	0.60
VMF	14.10	0.25	15.65	0.53
VMF + ION2	14.10	0.25	15.63	0.54
VMF + ION2 + AMB	14.09	0.25	15.62	0.54

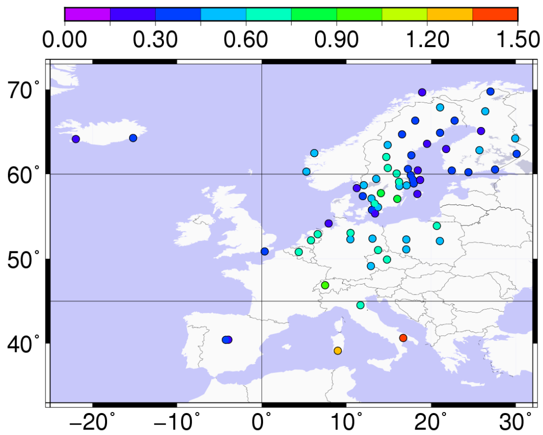

Figure 7. Estimated amplitudes of the diurnal cycle in the IWV at the 69 sites with more than 10 years of data.

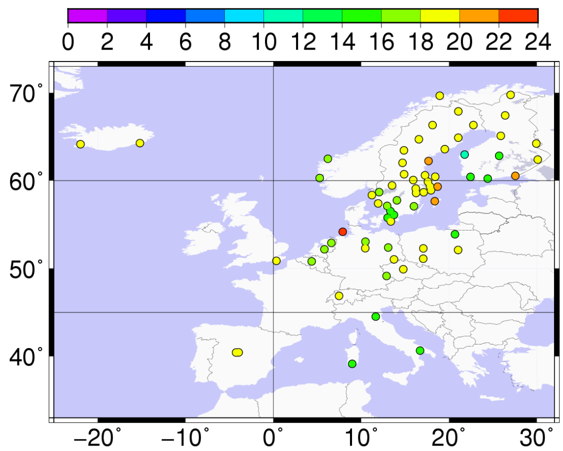

Figure 8. The peak of the hourly mean of the IWV in local solar time (same sites and time periods as in Figure 7).

Figure 8 depicts the peak time of hourly IWV mean. A trend is seen when we study the Scandinavian peninsula. The IWV peaks in the afternoon in the west and in the early night along the east coast.

4. CONCLUSION

We have compared the results obtained from two different data analyses in order to study the impact of the use of different models. We find that the impact is small, but the IWV results from different data analyses shall not be mixed when studying the long term stability of the IWV, e.g. when estimating trends.

Thereafter, we estimated linear trends and the diurnal cycle of the IWV from the analysis using the more recent models. The linear trends, estimated from the 35 sites having more than 15 years of data, show comparable values to their corresponding uncertainties which are rescaled in order to be consistent with the misfit of the model. In addition, clear differences are seen for the trends estimated for four difference seasons.

The estimated amplitude of the diurnal cycle is varying from 0.16 kg/m^2 to 1.46 kg/m^2 for the summer months (June, July, and August). The peak time of the hourly IWV mean is around 18 local solar time for the most of the sites and it shows a systematic variation from west to east of the Scandinavian peninsula.

REFERENCES

[1] Buehler, S.A., von Engeln, A., Brocard, E., John, V.O., Kuhn, T. & Eriksson, P. (2006). Recent developments in the line-by-line modeling of outgoing longwave radiation. J. Quant. Spectrosc. Radiat. Transfer, 98(3), 446–457, doi:10.1016/j.jqsrt.2005.11.001.

[2] Steigenberger, P., Tesmer, V., Krügel, M., Thaller, D., Schmid, R., Vey, S. & Rothacher, M. (2007). Comparisons of homogeneously reprocessed GPS and VLBI long time-series of troposphere zenith delays and gradients. J. Geod., 81(6-8), 503–514, doi:10.1007/s00190-006-0124-y.

[3] Ning, T., Elgered, G., Willén, U. & Johansson, J. M. (2013). Evaluation of the atmospheric water vapor content in a regional climate model using ground-based GPS measurements. J. Geophys. Res., 118, 329–339, doi:10.1029/2012JD018053.

[4] Niell, A. E. (1996). Global mapping functions for the

Table 3. Linear trends in the IWV for sites with more than 15 years of data for the different seasons and over all. The sites are sorted by increasing latitude.

Site	Latitude	Longitude	Winter	Spring	Summer	Autumn	All data
	°N	°E	kg/(m^2· decade)				
CAGL	39.1	9.0	0.29 ± 0.41	1.02 ± 0.44	0.00 ± 0.45	0.51 ± 0.46	0.43 ± 0.43
MATE	40.6	16.7	0.54 ± 0.40	0.84 ± 0.26	0.50 ± 0.36	0.29 ± 0.31	0.55 ± 0.31
WTZR	49.1	12.9	0.15 ± 0.35	0.36 ± 0.35	1.20 ± 0.38	0.38 ± 0.33	0.52 ± 0.29
BRUS	50.8	4.4	−0.71 ± 0.34	−0.98 ± 0.36	0.20 ± 0.40	0.47 ± 0.48	−0.25 ± 0.40
HERS	50.9	0.3	0.33 ± 0.34	0.13 ± 0.27	0.04 ± 0.33	1.42 ± 0.43	0.12 ± 0.36
JOZE	52.1	21.0	−0.13 ± 0.27	0.68 ± 0.34	1.70 ± 0.46	0.38 ± 0.35	0.58 ± 0.38
KOSG	52.2	5.8	−0.54 ± 0.44	−0.82 ± 0.55	0.69 ± 0.49	0.16 ± 0.48	−0.11 ± 0.42
BOR1	52.3	17.1	0.27 ± 0.27	0.56 ± 0.30	1.16 ± 0.38	0.20 ± 0.37	0.54 ± 0.35
WSRT	52.9	6.6	−0.38 ± 0.36	−0.72 ± 0.38	0.41 ± 0.43	−0.23 ± 0.45	−0.24 ± 0.39
LAMA	53.9	20.7	−0.48 ± 0.23	0.36 ± 0.24	1.60 ± 0.31	0.48 ± 0.39	0.52 ± 0.39
HAS0	56.1	13.7	−0.40 ± 0.26	0.01 ± 0.25	0.78 ± 0.28	0.20 ± 0.29	0.15 ± 0.28
OSK0	57.1	16.0	−0.40 ± 0.25	0.27 ± 0.27	0.55 ± 0.34	0.12 ± 0.34	0.15 ± 0.32
ONSA	57.4	11.9	−0.44 ± 0.27	0.23 ± 0.26	0.61 ± 0.29	0.45 ± 0.31	0.24 ± 0.32
VIS0	57.6	18.4	−0.46 ± 0.23	0.34 ± 0.29	0.71 ± 0.36	0.23 ± 0.33	0.22 ± 0.33
JON0	57.8	14.1	−0.49 ± 0.23	0.22 ± 0.25	0.60 ± 0.30	0.12 ± 0.30	0.13 ± 0.29
NOR0	58.6	16.2	−0.87 ± 0.29	0.58 ± 0.34	1.25 ± 0.44	−0.10 ± 0.46	0.25 ± 0.42
VAN0	58.7	12.0	−0.63 ± 0.24	0.20 ± 0.26	0.65 ± 0.30	−0.02 ± 0.33	0.06 ± 0.30
LOV0	59.3	17.8	−0.59 ± 0.21	0.58 ± 0.28	0.90 ± 0.33	0.19 ± 0.32	0.29 ± 0.31
KAR0	59.4	13.5	−0.57 ± 0.23	0.39 ± 0.27	0.79 ± 0.31	−0.05 ± 0.34	0.15 ± 0.31
METS	60.2	24.4	−0.71 ± 0.26	0.51 ± 0.43	−0.43 ± 0.44	0.84 ± 0.42	0.04 ± 0.41
MAR6	60.6	17.3	−0.45 ± 0.20	0.74 ± 0.27	0.82 ± 0.32	0.14 ± 0.32	0.33 ± 0.30
LEK0	60.7	14.9	−0.53 ± 0.18	0.45 ± 0.23	0.53 ± 0.27	−0.38 ± 0.29	0.03 ± 0.26
SVE0	62.0	14.7	−0.44 ± 0.16	0.49 ± 0.21	0.66 ± 0.28	−0.22 ± 0.27	0.15 ± 0.25
SUN0	62.2	17.7	−0.39 ± 0.18	0.65 ± 0.26	0.63 ± 0.32	−0.12 ± 0.33	0.21 ± 0.30
JOEN	62.4	30.1	−0.67 ± 0.25	0.37 ± 0.34	0.48 ± 0.54	0.86 ± 0.38	0.25 ± 0.41
VAAS	63.0	21.8	−0.53 ± 0.24	0.78 ± 0.30	0.74 ± 0.45	0.62 ± 0.43	0.37 ± 0.38
OST0	63.4	14.9	−0.22 ± 0.16	0.51 ± 0.22	0.40 ± 0.29	−0.12 ± 0.27	0.15 ± 0.26
UME0	63.6	19.5	−0.26 ± 0.18	0.58 ± 0.24	0.23 ± 0.34	−0.18 ± 0.34	0.11 ± 0.30
REYK	64.1	338.0	0.39 ± 0.28	−0.13 ± 0.30	−0.67 ± 0.31	−0.81 ± 0.32	−0.30 ± 0.31
HOFN	64.3	344.8	−0.06 ± 0.29	−0.80 ± 0.34	−1.20 ± 0.43	−0.94 ± 0.42	−0.78 ± 0.38
VIL0	64.7	16.6	−0.23 ± 0.27	0.45 ± 0.21	0.11 ± 0.29	0.02 ± 0.29	0.11 ± 0.26
SKE0	64.9	21.1	−0.24 ± 0.18	0.32 ± 0.23	−0.14 ± 0.33	−0.17 ± 0.35	−0.04 ± 0.30
ARJ0	66.3	18.1	−0.02 ± 0.15	0.36 ± 0.18	−0.03 ± 0.26	0.17 ± 0.26	0.13 ± 0.23
OVE0	66.3	22.8	0.01 ± 0.16	0.48 ± 0.21	0.04 ± 0.30	0.03 ± 0.30	0.15 ± 0.27
KIR0	67.9	21.1	0.05 ± 0.26	0.29 ± 0.19	−0.30 ± 0.27	0.04 ± 0.26	0.03 ± 0.23

atmosphere delay at radio wavelengths. J. Geophys. Res., 101, 3,227–3,246.

[5] Boehm, J., Werl, B. & Schuh, H. (2006). Troposphere mapping functions for GPS and very long baseline interferometry from European Centre for Medium-Range Weather Forecasts operational analysis data. J. Geophys. Res., 111, B02406, doi:10.1029/2005JB003629.

[6] Kedar, S., Hajj, G.A., Wilson, B.D. & Heflin, M.B. (2003). The effect of the second order GPS ionospheric correction on receiver positions. Geophys. Res. Lett., 30, 1829, doi:10.1029/2003GL017639

[7] Lyard F., Lefevre, F., Letellier, T. & Francis, O. (2006). Modelling the global ocean tides: Modern insights from FES2004. Ocean Dyn., 56, 394, doi:10.1007/s10236-006-0086-x.

[8] Nilsson, T. & Elgered, G. (2008). Long-term trends in the atmospheric water vapor content estimated from ground-based GPS data. J. Geophys. Res., 113, doi:10.1029/2008JD010110.

[9] Glowacki, T.J., Penna, N.T. & Bourke, W.P. (2006). Validation of GPS-based estimates of integrated water vapour for the Australian region and identification of diurnal variability. Aust. Met. Mag., 55, 131-148.